

Predictability of the 1997 and 1998 South Asian Summer Monsoons

Siegfried D. Schubert and Man Li Wu
Data Assimilation Office
Goddard Laboratory for Atmospheres
Greenbelt, Maryland

1 May 2000

To be submitted to J. Climate

Abstract

The predictability of the 1997 and 1998 south Asian summer monsoon winds is examined from an ensemble of 10 Atmospheric General Circulation Model (AGCM) simulations with prescribed sea surface temperatures (SSTs) and soil moisture. The simulations are started in September 1996 so that they have lost all memory of the atmospheric initial conditions for the periods of interest.

The model simulations show that the 1998 monsoon is considerably more predictable than the 1997 monsoon. During May and June of 1998 the predictability of the low-level wind anomalies is largely associated with a local response to anomalously warm Indian Ocean SSTs. Predictability increases late in the season (July and August) as a result of the strengthening of the anomalous Walker circulation and the associated development of easterly low level wind anomalies that extend westward across India and the Arabian Sea. During these months the model is also the most skillful with the observations showing a similar late-season westward extension of the easterly wind anomalies.

The model shows little predictability or skill in the low level winds over southeast Asia during 1997. Predictable wind anomalies do occur over the western Indian Ocean and Indonesia, however, over the Indian Ocean they are a response to SST anomalies that were wind driven and they show no skill. The reduced predictability in the low level winds during 1997 appears to be the result of a weaker (compared with 1998) simulated anomalous Walker circulation, while the reduced skill is associated with pronounced intraseasonal activity that is not well captured by the model. Remarkably, the model does produce an ensemble mean Madden-Julian Oscillation (MJO) response that is approximately in phase with (though weaker than) the observed MJO anomalies. This is consistent with the idea that SST coupling may play an important role in the MJO.

1. Introduction

A number of recent simulations of the Asian summer monsoon with atmospheric general circulation models (AGCMs) forced with observed sea surface temperatures (SSTs) suggest that a substantial fraction of the seasonal variability is not directly tied to remote forcing from El Niño-related SST anomalies in the central and eastern tropical Pacific (e.g. Arpe et al. 1998, Lau and Wu 1999; Soman and Slingo 1997; Ju and Slingo 1995; Lau et al. 1999). Lau et al. (1999) suggest that boreal spring warming in the North Arabian Sea and subtropical western Pacific may play a role in the development of a strong South Asian monsoon. Lau and Wu (1999) show that about 34% of the variability of the 1997-98 Asian-Australian northern summer monsoon is attributable to basin-scale SST influence associated with El Niño. Another 19% is attributable to regional coupled processes, and the remaining 47% is due to other factors such as high frequency transients.

Soman and Slingo (1997) show that for 1983 and 1984 the modulation of the Walker circulation (additional subsidence) is the dominant mechanism by which El Niño weakens the Asian summer monsoon, however, the delayed onset during El Niño may be associated with the complementary cold SST anomalies in the western Pacific which delay the northwards transition of the tropical convective maximum (TCM). They further suggest that during cold events it is primarily the warm SST anomalies in the western Pacific that enhance the TCM and lead to an early onset and stronger monsoon.

Lau and Wu (1999) note that India is not a major center of action in their dominant coupled precipitation-SST relationships. Arpe et al. (1998) studied the differences between 1987 and 1988 summer monsoons and suggest that, while the large scale dynamics over India are largely governed by Pacific SST, the variability of precipitation over India is impacted by a number of other factors including SST anomalies over the northern Indian Ocean, soil wetness, initial conditions, and the quasi-biennial oscillation. They show that the two direct effects of El Niño are to reduce precipitation over India and reduce the surface winds over the Arabian Sea. They suggest that the latter leads to an increase in SST and more precipitation over India acting to counteract the direct effect of El Niño. They further show a substantial seasonality of the predictability, with the model simulations and forecasts differing most during July when precipitation variability has no relationship to ENSO in their model simulation. They also show that the 1987/88 differences are of opposite sign in May and September and that this is reproduced in the simulations.

In this study, we present the results of an ensemble of 10 simulations of the 1997 and 1998 Asian summer monsoons with an AGCM forced with observed sea surface temperatures and soil moisture. The focus is on the interannual differences and seasonal evolution of the predictability of the monsoon winds. We are particularly concerned with the nature of the predictability and its link to local and remote SST forcing. Section 2 describes the AGCM and the simulations. An overview of the development of the 1997/98 ENSO and monsoon is given in Section 3. The results are presented in section 4, and the summary and conclusions are given in section 5.

2. The AGCM and Forecast Experiments

The AGCM is an early version of the Goddard Earth Observing System (GEOS-2) model described in (Chang et al. 2000). It has 43 sigma levels extending up to 10hPa and a horizontal resolution of 2° latitude by 2.5° longitude. The mean boreal winter extratropical ENSO response of this model is described in Chang et al. (2000).

For this study, we generate an ensemble of 10 simulations for the period 1 September 1996 through 31 August 1998. The simulations were carried out as part of the Asian-Australian Monsoon AGCM intercomparison project sponsored by the CLIVAR Asian-Australian Monsoon panel. Simulations were started from 10 independent 1 September initial conditions taken from several previously-completed long (1979-95) model simulations with prescribed monthly mean sea surface temperatures (SST). Beginning with 1 September 1996, the SST are prescribed from the weekly SST data of Reynolds and Smith (1994). Anomalies are computed with respect to a climatology computed from a single 13 year (1980-92) simulation with this version of the GEOS-2 model forced by observed monthly mean SSTs. It is important to note that this version of GEOS-2 did not have a land surface model. The prescribed soil moisture is determined from an off-line calculation using monthly mean observed precipitation and surface temperature (Schemm et al. 1992).

We use both the National Centers for Environmental Prediction (NCEP) climate data assimilation system (CDAS) and operational European Center for Medium Range Weather Forecasts (ECMWF) analyses for validation (the choice of which to use is based on the in-house availability of the analyses). While these data (especially the velocity potential fields) are clearly impacted by deficiencies in the assimilating models we shall, for brevity, occasionally refer to them as the observations.

3. Background: The 1997/98 ENSO and Monsoon

The 1997 Asian summer monsoon developed during the early stages of a major El Niño event. During May, the average anomaly in the Niño 1+2 region had reached 2.9°C and strong low level westerly anomalies were observed just west of the dateline (CPC 1997). Tropical convection was enhanced over the central equatorial Pacific, much of the central Indian Ocean extending over Australia, and suppressed from the eastern Indian Ocean eastward to the western Pacific. During June, the low level westerly wind anomalies extended across much of the equatorial Pacific Ocean and northwestward to the coast of China. Large easterly and northeasterly low level wind anomalies occurred over the Indian Ocean acting to suppress the development of the southwest monsoon. A weakened Somali jet led to reduced cold water upwelling and warm SST anomalies in the western Indian Ocean. Convection was reduced over Indonesia extending to southeast India, while it was enhanced over the eastern equatorial Pacific and the western Indian Ocean extending to northwest India.

During July of 1997, substantial warming occurred over much of the Indian Ocean (Webster et al. 1998b; Murtugudde et al. 1999). The warming continued into 1998 with unprecedented February 1998 SST anomalies of 1.5-2 degrees in the western Indian Ocean. SST anomalies exceeding 1° continued well into the beginning of the monsoon season (May and June 1998). The 1997 July low level wind anomalies were much reduced from the June values over the Pacific and Indian Oceans (CPC 1997). Also in contrast to June, convection was near normal over much of Indonesia and IndoChina as a result of intraseasonal activity during this month. During August, low level westerly anomalies strengthened in the central equatorial Pacific: these extended to the northwest to IndoChina, with very weak anomalies extending even further west across India. Reduced convection returned over much of Indonesia together with enhanced convection to the north extending into the South China Sea. Anomalous large scale sinking motion was largely confined to the southeast Indian Ocean in a region centered on 100°E , 15°S . Strong cooling was evident in the eastern Indian Ocean from September – January 1997/98, with surface easterlies replacing the climatological westerlies along the equator (Murtugudde et al. 1999). Considerable month-to-month variability in the ENSO indices suggest a strong impact from intraseasonal (MJO) activity, which had been prevalent since February 1996 (CPC 1997). In fact, the 1997 southwest monsoon developed over much of Indo-China and the Bay of Bengal during an active phase of the 30 to 60-day intraseasonal oscillation (ISO) in May. Another active phase of the ISO was evident at the end of June (Cleland 1998).

The 1998 Asian summer monsoon developed at a time of transition of the 1997/98 ENSO from warm to cold conditions. Troup's Southern Oscillation Index (SOI) went from -25 in April 1998 to zero in May and to $+10$ in June (Courtney 1998). During May convection over the equatorial Indian and Pacific Oceans was more variable than observed during the past year, possibly associated with the MJO (CPC 1998). Precipitation was near normal over India and Indonesia. SSTs remained above normal over the Indian Ocean during May and June. During June tropical convection was above normal over Indonesia for the first time in over one year. Rainfall was near normal over India, though it was above normal in the southern Bay of Bengal and the Arabian Sea. Low level easterly wind anomalies were confined to the western Pacific east of 90°E

During July, SSTs remained above normal in the eastern Pacific and Indian Ocean (CPC 1998). Tropical convection was suppressed across the western equatorial Pacific Ocean and parts of Indo-China and the Bay of Bengal, and enhanced to the south across Indonesia and the eastern Indian Ocean. Convection and rainfall remained near normal over India. Both June and July had upper level westerly wind anomalies across the western and central equatorial Pacific Ocean in association with an anomalous subtropical cyclone just south of the equator near the dateline. The associated low level easterly wind anomalies extend from the central Pacific across Indonesia, the Bay of Bengal and India, acting to suppress the further development of the southwest monsoon. Indian Ocean SSTs remained anomalously warm in August. Tropical convection was suppressed across the western and central Pacific Ocean and enhanced across Indonesia and the eastern Indian Ocean (this pattern developed during June and persisted for 3 months). Rainfall was slightly above normal over India. The low level easterly anomalies in the western Pacific now extend westward well into the Bay of Bengal, with the upper level cyclone now situated over Australia.

4. Results

In this section we present the results of the model simulations and compare them with the observations. We define predictability in terms of the agreement among the ten ensemble members of the model simulations. We define skill in terms of the agreement between the observations and ensemble mean of the simulations. The former is a property only of the model and the boundary forcing, while the latter measures both predictability and the veracity of the model simulations.

Figure 1 shows the evolution of the 850hPa winds determined from the operational ECMWF analyses. The corresponding model results are shown in Fig. 2 for the mean of all 10 ensemble members. The format of these figures follows that of Webster et al. 1998a and highlights the seasonal development of the Asian monsoon. The model produces a realistic evolution of the

monsoon winds over the Indian Ocean characterized by the development of southerlies (cross-equatorial flow) and the low level westerlies north of the equator in early May. The observations show a suppressed development of the westerlies west of 90° during June 1997 as mentioned in the previous section. This is not evident in the model simulation. Both the model and simulations show westerlies extending well east of 135°E during the warm event, while they are generally confined west of 135°E during 1998. The westerlies remain strong throughout the warm season, with substantial intraseasonal variations evident in the observations. While this is less evident in the ensemble mean of the model simulations, we do find similar intraseasonal variability in the individual ensemble members (not shown). The transition from westerlies to easterlies in October marks the end of the monsoon season in both the model and observations.

While the model produces a very realistic evolution of the low level monsoon winds, there is a tendency for the model wind fluctuations to be weaker than the observed. While this is to be expected in the ensemble mean fields shown in Fig. 2, we find this to be also true for the individual ensemble members. The weaker variability in the model, and its impact on predictability estimates will be discussed further in the conclusions.

We next focus on the differences between the 1997 and 1998 monsoon winds. As mentioned above, the 1997 monsoon developed during the initial phase of a major warm event, while the 1998 monsoon developed during a transition from warm to cold conditions. The 1998-1997 monthly mean 850hPa wind differences are shown in Fig. 3 for the AGCM ensemble mean (left panels) and the observations (right panels). During May the AGCM shows significant westerly differences over the eastern Indian Ocean with a cyclonic circulation over the Arabian Sea. Easterly differences occur over Indonesia with confluence over the central Indian Ocean. The observations show generally weaker differences though they are generally not inconsistent with the simulations. The SST field shows positive differences exceeding 1°C in the equatorial region just south of India. A comparison of the SST differences with the ensemble mean 850hPa wind differences suggests that the signal in the wind is primarily a response to the warm SSTs. This is examined further in Figs. 4 and 5, which show the individual 1998 and 1997 anomalies, respectively. During May 1997 the simulation shows few areas with a significant response. In fact, the ensemble mean May difference field is dominated by the 1998 anomalies, at a time of substantial warm SST anomalies in the Indian Ocean (Fig. 4).

The June 1998-1997 850hPa wind difference maps (Fig. 3) show significant simulated westerly wind differences in the equatorial western Indian Ocean. The observed differences, on the other hand, show westerlies extending across the Indian Ocean and a cyclonic circulation over India and

the surrounding regions. Comparisons with the 1998 and 1997 anomalies in Figs. 4 and 5, suggest that the simulation is responding to the 1998 warm SST anomalies in the western Indian Ocean (Figure 4), while the observed difference maps reflect primarily a strong suppression of the Somali jet during June of 1997. This is accompanied by a warming of the western Indian Ocean apparently as a result of reduced upwelling (Murtugudde et al. 1999). In fact the simulated June 1997 anomaly in the western Indian Ocean is southeasterly (instead of the observed northwesterly) suggesting the model is responding to the wind driven SST anomalies. Significant easterly anomalies occur over Indonesia and Indochina during both 1998 and 1997. These are not inconsistent with the observations.

July and August are characterized by large regions of significant ensemble mean 850hPa 1998-1997 wind differences (Fig. 3). Both months are characterized by easterly wind anomalies extending from the western Pacific north of the equator across Indochina and northern India. Westerly anomalies occur across much of the tropical Indian Ocean and Indonesia. The observations show a generally similar pattern of differences in the winds, with generally easterly anomalies north of the equator and a tendency for westerly anomalies to the south. Substantial differences exist, however, in the detailed structure and location of the observed and simulated differences. During these two months an extensive area of positive SST differences ($> 1^{\circ}\text{C}$) occurs east of about 90°E . Large negative differences ($< 1^{\circ}\text{C}$) are confined to a region just off the equatorial east coast of Africa. A comparison with the wind anomalies (Figs. 4 and 5) shows that the ensemble mean difference fields to a large extent reflect the 1998 anomalies. The 1997 simulated anomalies (Figure 5) tend to be of opposite sign to the 1998 anomalies to the east of 90° . On the other hand, the 1997 wind anomalies in the western Indian Ocean continue to reflect the anomalous SST in the western Indian Ocean and Arabian Sea.

In order to better quantify the predictability and skill of the AGCM simulations, we compute the spatial correlations between various 850hPa wind difference maps for the monsoon region (30°E - 120°E , 20°S - 30°N). Fig. 6 shows the spatial correlation between all pairs of the 1998-1997 difference maps for the 10 members of the ensemble for the two wind components (black dots). If the differences were completely random the dots would be scattered throughout the four quadrants of the plot. A highly predictable signal would have all the points clustered in the upper right hand corner (all correlations near one). The model results show a tendency for the dots to fall along a line in the upper right hand quadrant suggesting the interannual differences are predictable, though some of the correlations are close to zero. July and August show greater predictability in the zonal wind differences. This is consistent with the large regions of significant ensemble mean differences during these months shown in Fig. 3. The green dots show the correlations between

each ensemble member and the ensemble mean. The red dot is the correlation between the ensemble mean and the observations and measures the skill of the model simulations. The extent to which the red dot is an outlier from the green dots is an indication of model and/or forcing deficiencies. That is, for a perfect model and perfect forcing (e.g. SST and soil moisture), the observed “realization” should be statistically indistinguishable from any of the members of the ensemble.

The enhanced predictability of the low level zonal winds during July and August is associated with the strengthening of the anomalous Walker circulation during the mature phase of the 1998 monsoon season. This is evident from Fig. 7, which shows the seasonal development of the upper level velocity potential anomalies. Both the model (left panels of Fig. 7) and observations (right panels of Fig. 7) show an increased tendency for sinking motion over the Pacific during the course of the summer season. There is also a tendency for increased anomalous rising motion over the Indian Ocean in the simulations, though this is less evident in the observations.

Figure 8 shows the 3-dimensional structure of the anomalies during July and August of 1998. The model simulations (left panels of Fig. 8) show that the low level easterly anomalies over south Asia are part of a larger-scale circulation anomaly consisting of an anomalous upper level (low level) cyclonic (anticyclonic) couplet straddling the equator over the western Pacific. Low level convergence occurs along a line extending from the Arabian Sea to Indonesia. The corresponding anomalous Walker circulation shows a tendency for enhanced rising motion over the Indian Ocean and sinking motion over the central Pacific as discussed above. The observations (right panels of Fig. 8) are not inconsistent with the model results, though the main features discussed above are somewhat noisier. In particular, the broad region of anomalous sinking motion over the Pacific is less well defined compared with the simulation. The upper level cyclonic couplet is also less well defined particularly north of the equator. At low levels the easterly anomalies over south Asia do not extend as far to the northwest as in the simulations. The lower right panel of Fig. 8 shows the anomalous SSTs during July and August. The anomalously cold equatorial SSTs east of the dateline associated with the developing cold event are clearly evident. Warm SST anomalies occur over much of the Indonesian sector and eastern Indian Ocean.

The evolution of the Walker circulation during 1997 (Fig. 9) is considerably different from that of 1998 (Fig. 7). In addition to the generally opposite sense of the anomalies (anomalous rising motion over the eastern Pacific and anomalous sinking motion west of the dateline associated with the warm event), there is considerably more month to month variability, especially in the observations. For example, during June the anomalous sinking motion is particularly strong over

Indonesia. This occurs at a time when the development of the Somali Jet is inhibited (Fig. 5). On the other hand, during July the anomalous sinking motion is much reduced with generally small anomalies in the velocity potential over much of south Asia. The simulations show a tendency for a similar behavior though not nearly as strong. For example, the enhanced sinking motion over Indonesia in June, is also evident in the simulations, though with much reduced amplitude. It is also noteworthy that the descending branch of the anomalous Walker circulation during July and August occurs over the southern Indian Ocean well south of India.

The large month-to-month variability described above appears to be the result of unusual intraseasonal variability associated with the MJO. The right panel of Fig. 10 shows a time-longitude section of the “observed” daily velocity potential fields as determined from the NCEP CDAS. The observations show evidence for substantial MJO activity during the first half of 1997, with well defined propagating anomalies occurring during the period March through July. Remarkably, there is a signature of these events in the ensemble mean of the model simulations (left panel of Fig. 10). This suggests that the model is responding to the signature of the MJO in the weekly SST observations. We note that the model is also forced by an estimate of the observed soil moisture (see section 2), though these are monthly means, and so it is unlikely that they play a role in these events as suggested by Webster (1995). During 1998, the model shows a stationary development of the upper level velocity potential anomalies in response to the emerging cold event with a transition from negative to positive anomalies occurring near 110°E. The observations, on the other hand, show a tendency for the negative anomalies to propagate slowly to the east during 1998.

5. Summary and Conclusions

This study examined the predictability of the 1997 and 1998 south Asian summer monsoons from an ensemble of 10 AGCM simulations with prescribed SSTs and soil moisture. The simulations were started in September 1996 so that they have lost all memory of the atmospheric initial conditions for the periods of interest. Results were presented for each month (May-August) for the monsoon region (30°E-120°E and 20°S-30°N). The focus was on the predictability of the 850hPa winds.

The model simulations show pronounced interannual and seasonal differences in predictability. During May and June of 1998 the predictability of the low level wind anomalies is largely associated with a local response to the anomalously warm Indian Ocean SSTs during 1998. Such a local response is also evident in the observations during May. During June of 1997 the observed

wind anomalies are dominated by a reduction in the strength of the Somali jet associated with the developing warm event. In contrast, the model wind anomalies reflect a local response to the warming of the western Indian Ocean that is associated in part with the reduced upwelling in that region. This highlights a problem with prescribed SST experiments since in nature the western Indian Ocean SST anomalies during June 1997 are apparently forced by the wind anomalies.

The increase in predictability during 1998 occurs late in the season (July and August) as a result of the strengthening of an anomalous Walker circulation (centered on about 140°E with rising motion over the Indian Ocean and sinking motion over the central Pacific) and the associated development of easterly low level wind anomalies that extend westward across India and the Arabian Sea. During these months the model is also most skillful with a similar extension of the easterly wind anomalies occurring in the observations. During 1997 the simulated anomalous Walker circulation is of opposite sign, but weaker in amplitude compared to 1998. The model shows little skill during 1997. This appears to be the result of the weaker anomalous Walker Circulation, and pronounced intraseasonal activity associated with the MJO.

Remarkably, the model produces an ensemble mean MJO response that is approximately in phase with (though weaker than) the observed MJO anomalies. It is unlikely that these are forced by the imposed soil moisture anomalies since these are specified on a monthly basis. We speculate that the simulated events are responding to the imposed weekly SST anomalies that developed as part of the observed MJO variations. As such, the sensitivity of the model simulations to such SST anomalies is consistent with the idea that SST coupling may play an important role in the MJO. Further analysis of these events is on-going, and will be reported on as part of a separate study.

The results presented here are clearly model dependent. The GEOS-2 model, for example, appears to have a weak ENSO response in the extratropics during boreal winter (Chang et al. 2000). To the extent that is also true during summer and the monsoon region, the results presented here may give an underestimate of the ENSO-related predictability of the monsoon. On the other hand, a weak MJO signal and the general tendency for weaker than observed intraseasonal variability characteristic of this and other AGCMs, would tend to produce unrealistically optimistic estimates of predictability. We are currently addressing the issue of model dependence by conducting an intercomparison of a number of different AGCM simulations of the 1997/98 monsoons as part of the CLIVAR Asian-Australian Monsoon AGCM intercomparison project.

Acknowledgements: We wish to thank Chung-Yu Wu and Yehui Chang for carrying out the model integrations. We also thank Ching-I Lin for help with the data processing. This work was supported by the NASA Earth Science Enterprise's Global Modeling and Analysis Program, and the NASA Seasonal-to-Interannual Prediction Project.

References

- Arpe, K., L. Dumenil, and M.A. Giorgetta, 1998: Variability of the Indian Monsoon in the ECHAM3 model: sensitivity to sea surface temperature, soil moisture, and the stratospheric quasi-biennial oscillation. *J. Climate*, 11, 1837-1858.
- Chang, Y., S.D. Schubert, M.J. Suarez, 2000: Boreal winter predictions with the GEOS-2 GCM: The role of boundary forcing and initial conditions. *Quart. J. Roy. Met. Soc.*, to appear.
- Cleland, S.J. 1998: The tropical circulation in the Australian/Asian region-May to October 1997. *Aust. Met. Mag.*, 47, 71-81.
- Climate Prediction Center, 1997: Climate Diagnostics Bulletin, April – September 1997. NOAA/National Weather Service, National Centers for Environmental Prediction, Camp Springs, MD.
- Climate Prediction Center, 1998: Climate Diagnostics Bulletin, April – September 1998. NOAA/National Weather Service, National Centers for Environmental Prediction, Camp Springs, MD.
- Courtney, J. 1998: Seasonal climate summary southern hemisphere (autumn 1998): decline of a warm episode (El Nino). *Aust. Met. Mag.* 47, 339-346.
- Ju, J. and J. Slingo 1995: The Asian summer monsoon and ENSO. *Quart. J. Roy. Meteor. Soc.*, 121, 1133-1168.
- Lau, K.-M., K.-M. Kim, and S. Yang, 1999: Dynamical and boundary forcing characteristics of regional components of the Asian summer monsoon. Submitted to *J. Climate*.
- Lau, K.M. and H.-T. Wu, 1999: Assessment of the impacts of the 1997-98 El Nino on the Asian-Australia monsoon. *Geophys. Res. Letters*, 26, 1747-1750.
- Murtugudde, R., J.P. McCreary, Jr., A.J. Busalacchi, 1999: Oceanic processes associated with anomalous events in the Indian Ocean with relevance to 1997-98. *J. Geophys. Res.*,

Reynolds, W. R. and T. M. Smith, 1994: Improved global sea surface temperature analyses using optimum interpolation. *J. Climate*, 7, 929 -948.

Schemm, J.-K., S. Schubert, J. Terry, S. Bloom and Y. Sud, 1992: Estimates of monthly mean soil moisture for 1979-89, NASA Tech. Memo. No. 104571, Goddard Space Flight Center, Greenbelt, MD 20771.

Soman M.K. and J. Slingo, 1997: Sensitivity of the Asian monsoon to aspects of sea-surface -temperature anomalies in the tropical Pacific Ocean. *Q.J.R. Meteorol. Soc.*, 123, 309-336.

Webster, P.J. 1995: Role of hydrological processes in ocean-atmosphere interactions. *Rev. Geophys.*, 32, 427-476.

Webster, P.J., T. Palmer, M. Yanai, V. Magana, J. Shukla, and T. Yasunari, 1998a: Monsoons: Processes and predictability and prospects for prediction. *J. Geophys. Res. Special Issues*, 103 (C7), 14451-14510.

Webster, P.J., J. Loschnigg, A. Moore and M. Reban, 1998b: The great 1997-1998 warming of the Indian Ocean: Evidence of coupled ocean-atmosphere instabilities. *Nature*

List of Figures

Figure 1: Longitude-time plots of the daily 850hPa winds from the ECMWF operational analyses. Left panel: Meridional wind averaged between 5°S and 5°N. Middle panel: Zonal wind averaged between 5°N and 10°N. Right Panel: Zonal wind averaged between 5°S and 10°S. Units are m/s.

Figure 2: Same as Figure 1, except from the ensemble mean of the 10 AGCM simulations.

Figure 3: Left panels: Simulated 850hPa ensemble mean monthly mean wind difference (1998-1997) maps. Right panels: Observed 850hPa monthly mean wind difference (1998-1997) fields superimposed on the SST differences for May, June, July and August. The simulated wind vectors are color coded to indicate significance at the 5% level. Red (blue) indicates that only the u (v) component is significant. Green (black) indicates that both (neither) components are significant. Units are m/s for the wind and °C for the SSTs.

Figure 4: Left panels: Simulated 850hPa ensemble mean monthly mean wind anomalies for 1998. Right panels: Observed 850hPa monthly mean wind anomalies for 1998 superimposed on the SST anomalies for May, June, July and August. The simulated wind vectors are color coded to indicate significance at the 20% level. Red (blue) indicates that only the u (v) component is significant. Green (black) indicates that both (neither) components are significant. Units are m/s for the wind and °C for the SSTs.

Figure 5: Same as Figure 4, except for 1997.

Figure 6: 1998-1997 850hPa wind difference correlation scatter plots for May, June, July and August. The green dots are the spatial correlations between the ensemble mean and each individual ensemble member. The red dot is the correlation between the ensemble mean and observations (ECMWF analysis). The black dots are the correlations between all pairs of ensemble members.

Figure 7. Monthly mean velocity potential anomalies for 1998. Left panels: the ensemble mean AGCM simulation. Right panels: the ECMWF analyses. Units are $10^6 \text{ m}^2\text{s}^{-1}$.

Figure 8: Left panels: The upper panel shows the simulated 200hPa ensemble July/August mean wind and velocity potential anomalies for 1998. The lower panel shows the ensemble July/August mean 850hPa wind anomalies. The wind vectors are color coded to indicate significance at the 10% level. Red (blue) indicates that only the u (v) component is significant. Green (black)

indicates that both (neither) components are significant. Right panels: The upper panel shows the observed (ECMWF analyses) 200hPa July/August mean wind and velocity potential anomalies for 1998. The lower panel shows the observed July/August mean 850hPa wind and SST anomalies. The arrow in the lower right corner indicates a wind anomaly of 8m/s. Contour intervals for velocity potential are $-9 -7 -5 -3 -1 1 3 5 7 9 10^6 \text{ m}^2\text{s}^{-1}$. Units for the SST are $^{\circ}\text{C}$.

Figure 9. Same as Figure 7, except for 1997.

Figure 10: Time-longitude diagram of the 200hPa velocity potential anomalies averaged between 5°N and 10°N computed from the ensemble mean AGCM simulations (left panel), and NCEP analyses (right panel). Values plotted are 5-day averages. Units are $10^6 \text{ m}^2\text{s}^{-1}$.

Observations
(Wind (ms^{-1}) at 850 hPa)

V (5S-5N)

U (5N-10N)

U (10S-5S)

Aug 98
Jul 98
Jun 98
May 98
Apr 98
Mar 98
Feb 98
Jan 97
Dec 97
Nov 97
Oct 97
Sep 97
Aug 97
Jul 97
Jun 97
May 97
Apr 97
Mar 97
Feb 97
Jan 97
Dec 96
Nov 96
Oct 96
Sep 96

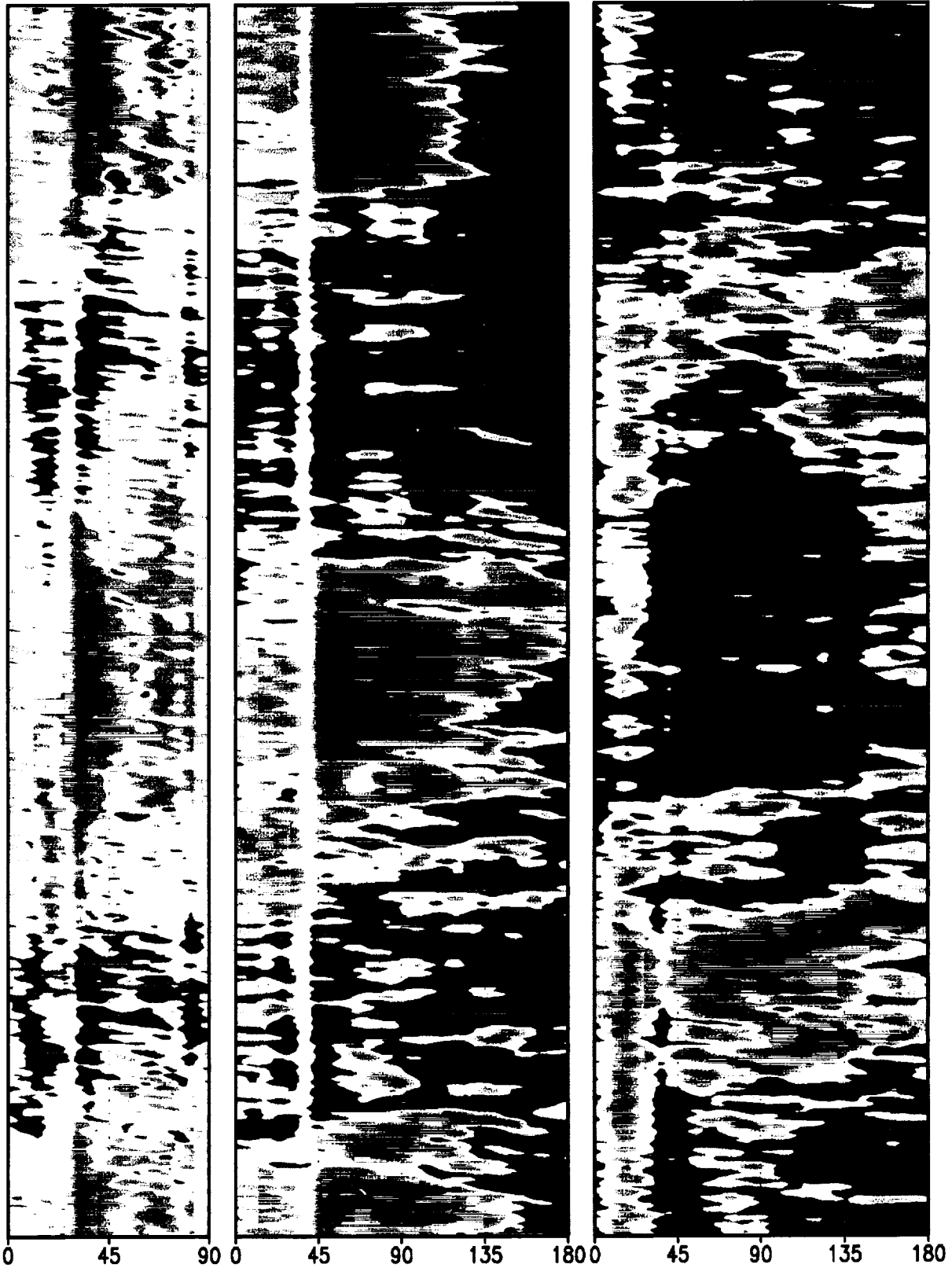


Fig. 1

-20 -16 -12 -8 -4 4 8 12 16 20

Ensemble Mean Simulation
(Wind (ms^{-1}) at 850 hPa)

V (5S-5N)

U (5N-10N)

U (10S-5S)

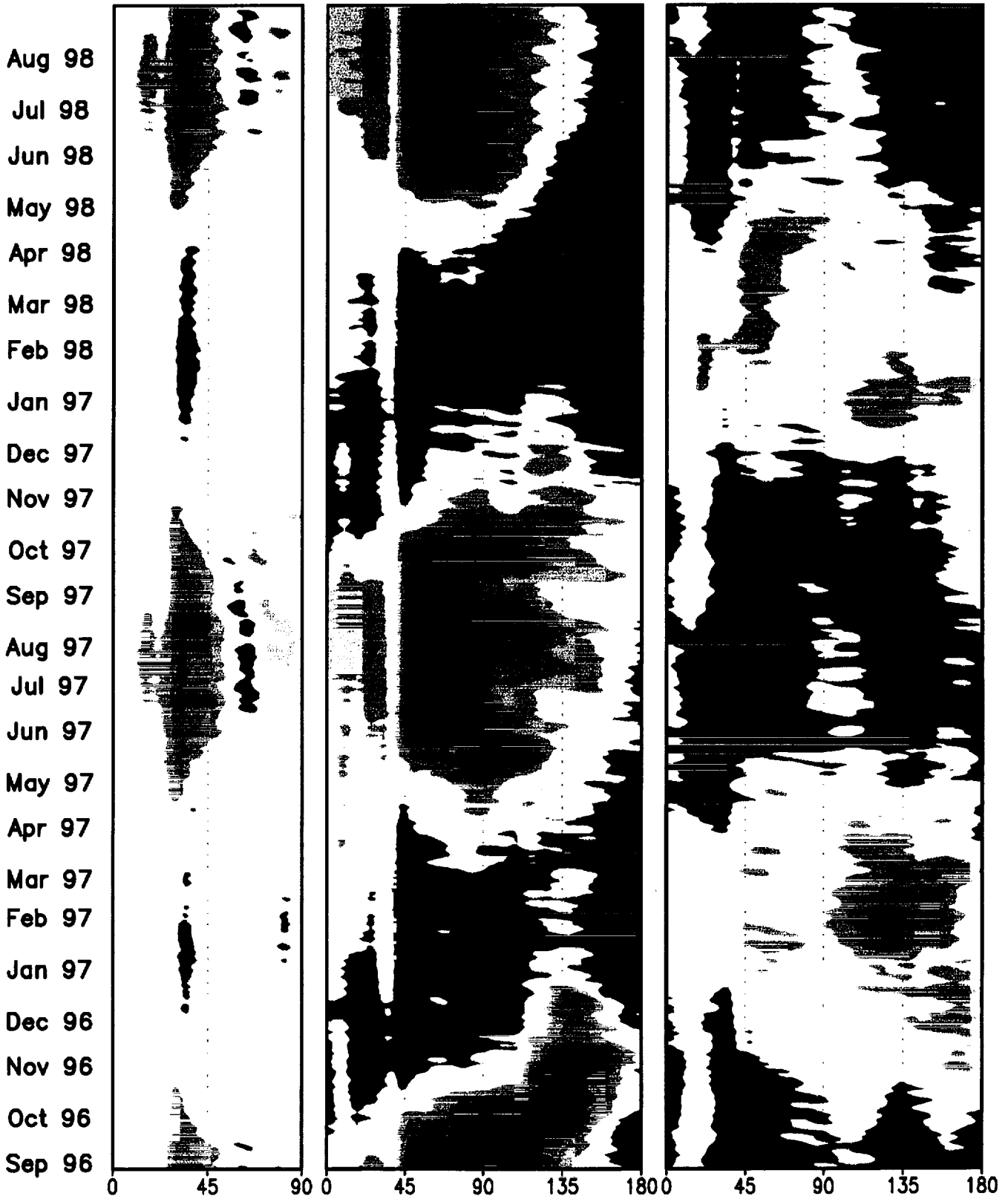
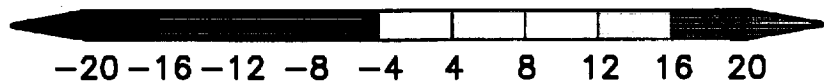


Fig. 2



Wind Differences (1998 minus 1997) at 850 hPa (ms^{-1})
and SST Differences ($^{\circ}\text{C}$)

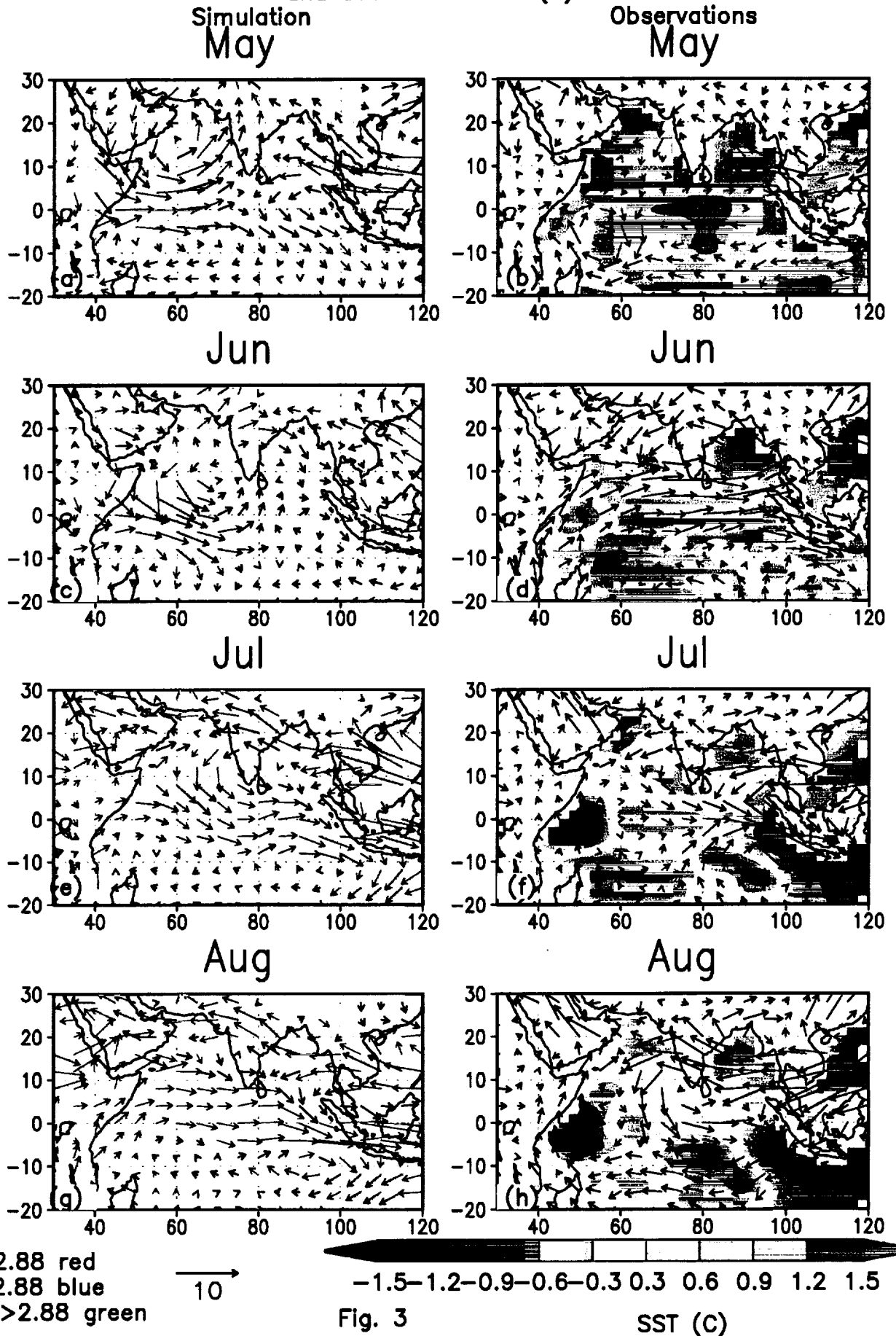


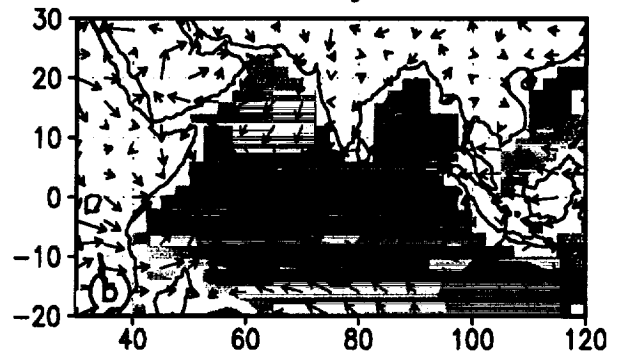
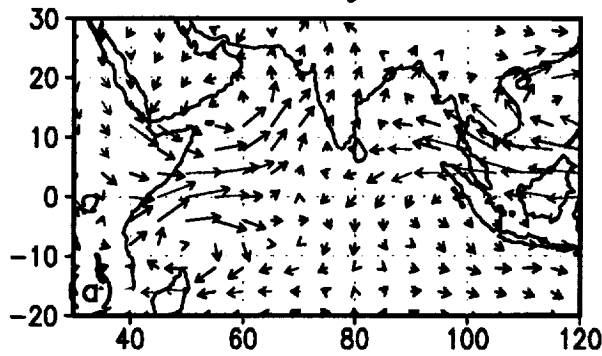
Fig. 3

SST ($^{\circ}\text{C}$)

Wind Anomalies (ms^{-1}) at 850 hPa and SST Anomalies ($^{\circ}\text{C}$)
(1998)

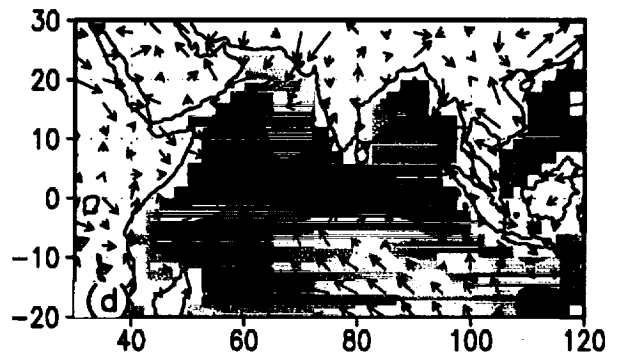
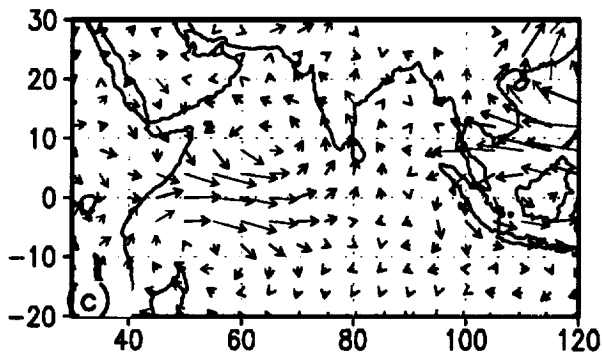
Simulation
May

Observations
May



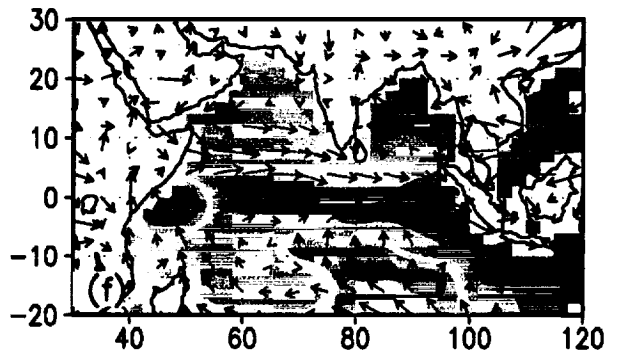
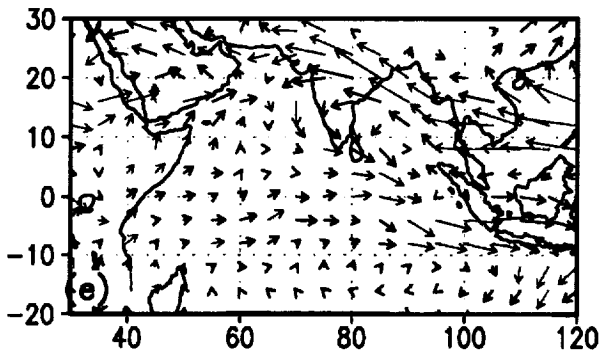
Jun

Jun



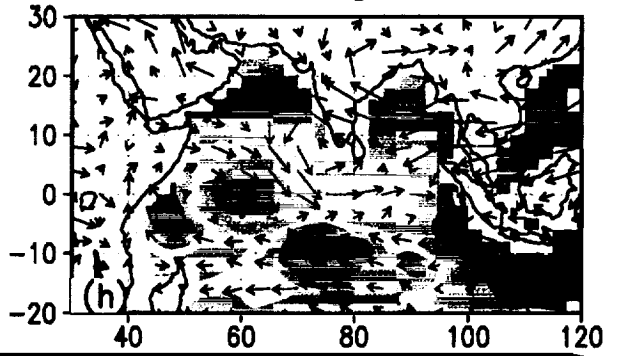
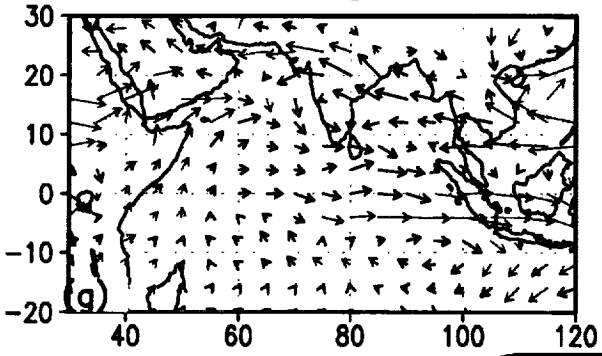
Jul

Jul



Aug

Aug



$u > 1.38$ red
 $v > 1.38$ blue
 $u, v, > 1.38$ green



-1.2 -0.9 -0.6 -0.3 -0.1 0.1 0.3 0.6 0.9 1.2

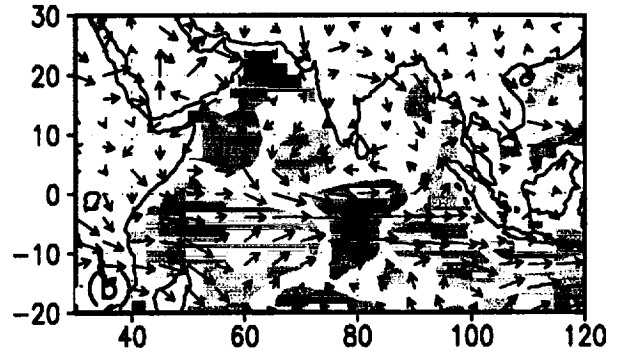
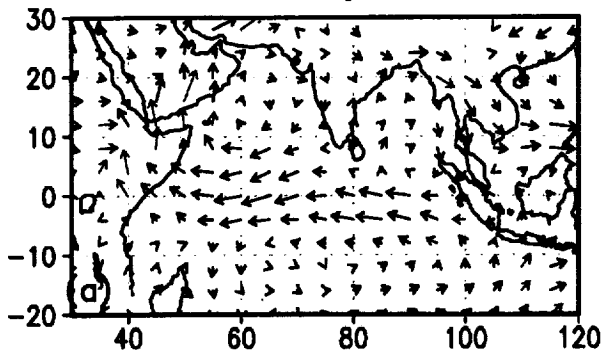
SST ($^{\circ}\text{C}$)

Fig. 4

Wind Anomalies (ms^{-1}) at 850 hPa and SST Anomalies ($^{\circ}\text{C}$)
 (1997)

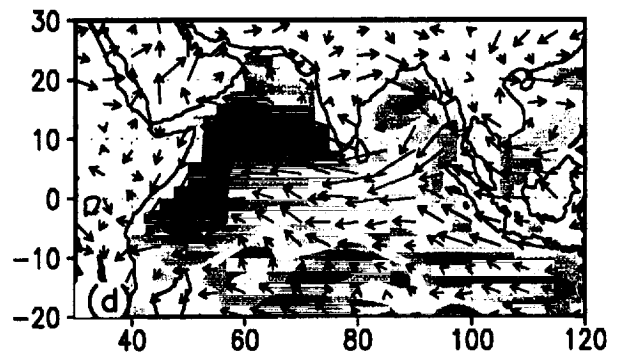
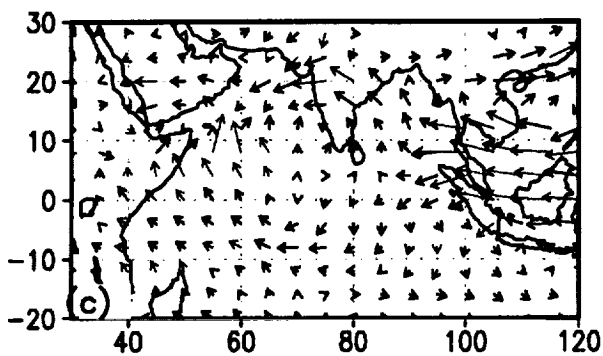
Simulation
 May

Observations
 May



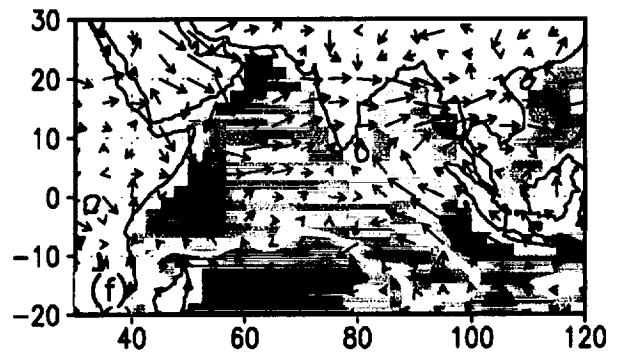
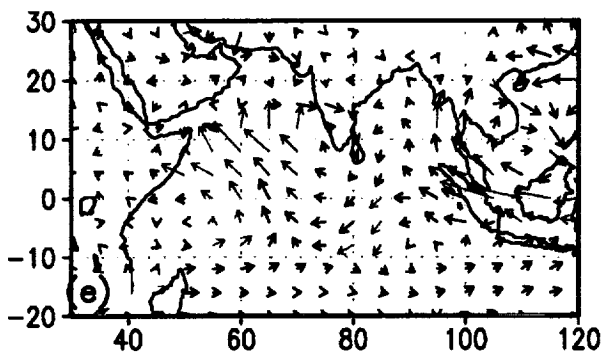
Jun

Jun



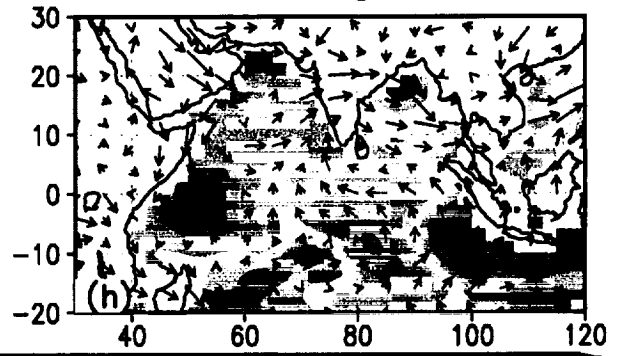
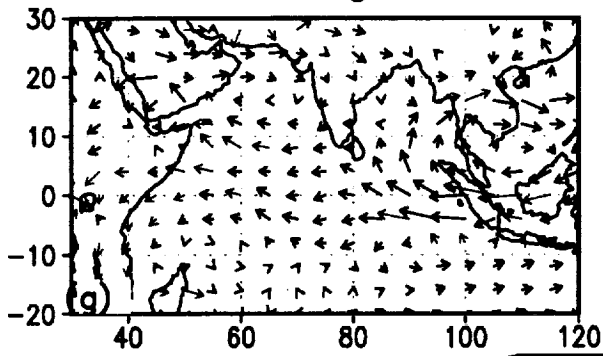
Jul

Jul



Aug

Aug



$u > 1.38$ red
 $v > 1.38$ blue
 $u, v, > 1.38$ green

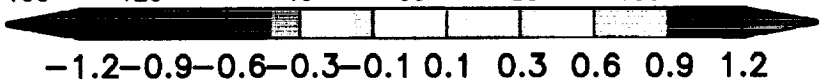


Fig. 5

SST ($^{\circ}\text{C}$)

Pattern Correlation
(30E to 120E; 20S to 30N)
Wind Differences (1998 minus 1997) at 850 hPa

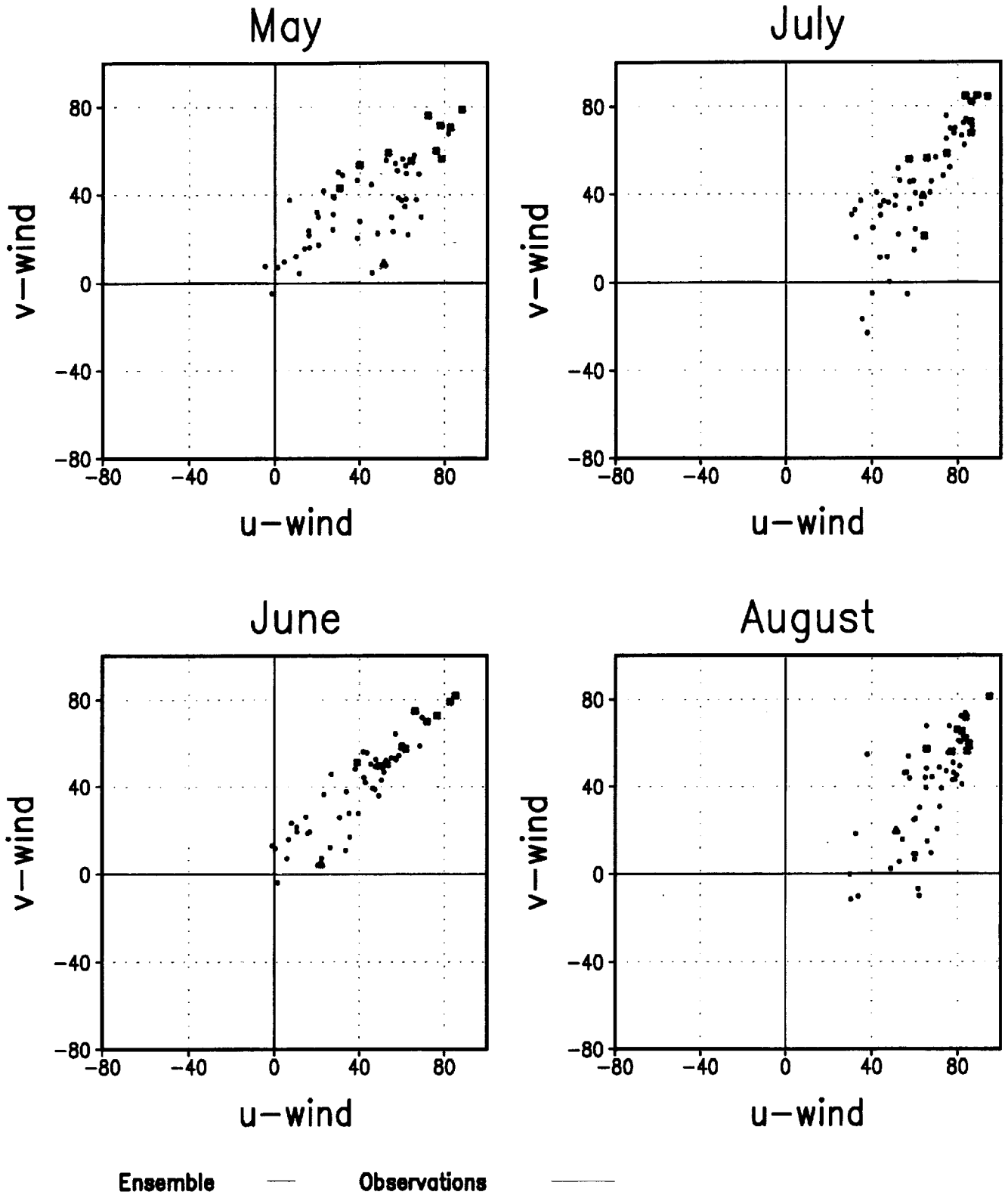
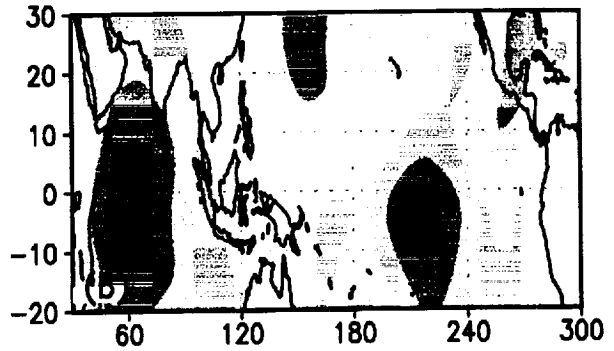
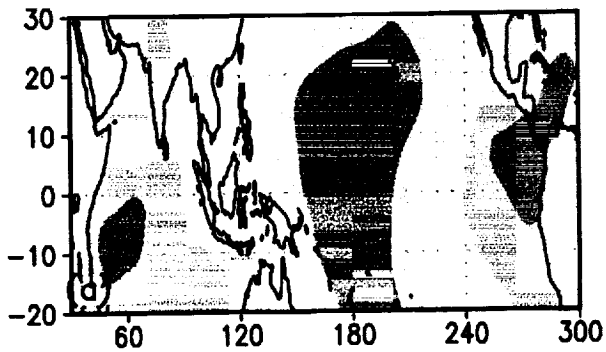


Fig. 6

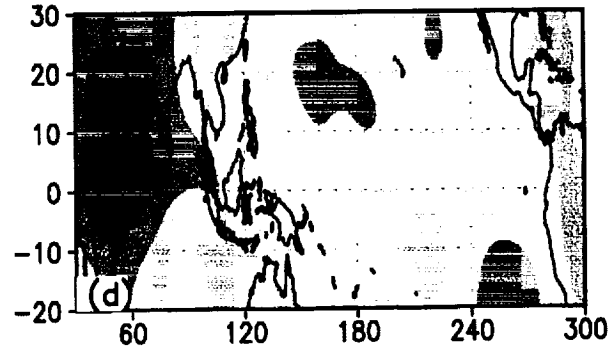
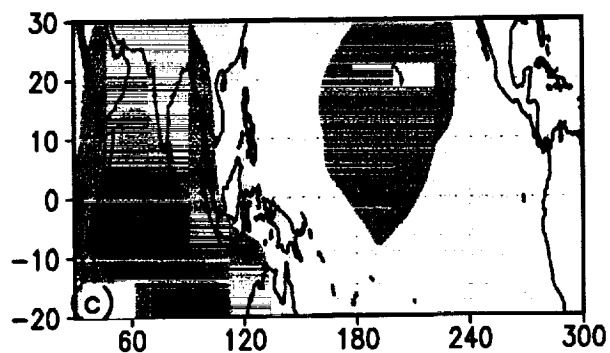
Velocity Potential at 200 hPa ($10^{-6}m^2s^{-1}$)
(1998)

Simulation Observations
May May



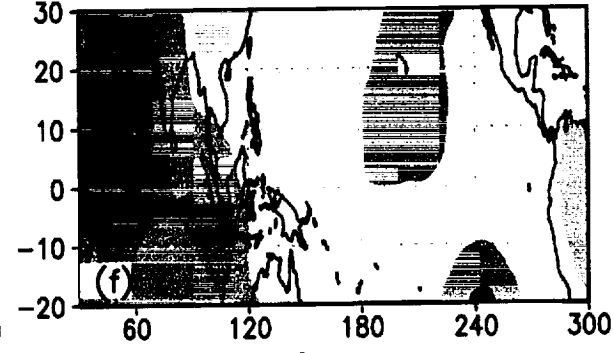
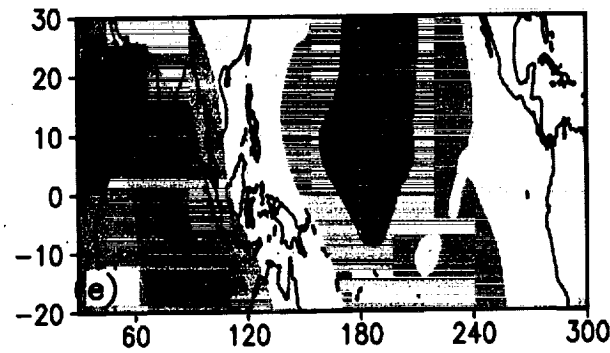
Jun

Jun



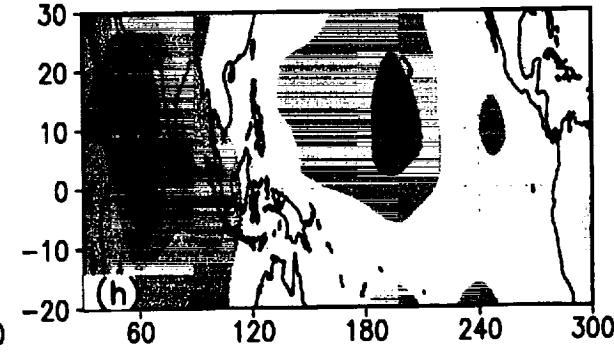
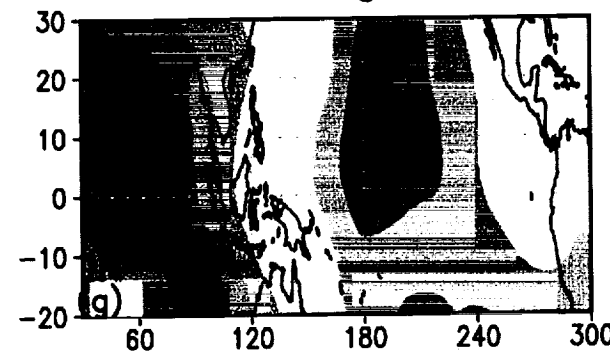
Jul

Jul



Aug

Aug

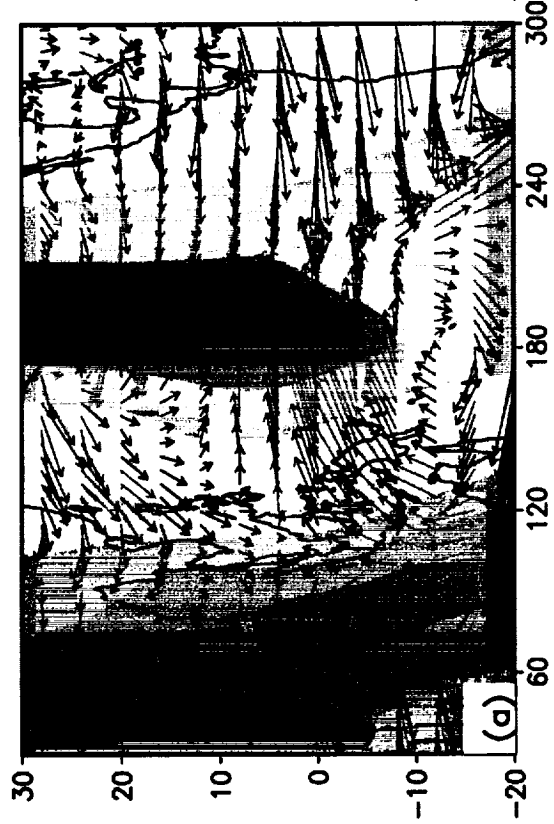


-9 -7 -5 -3 -1 1 3 5 7 9

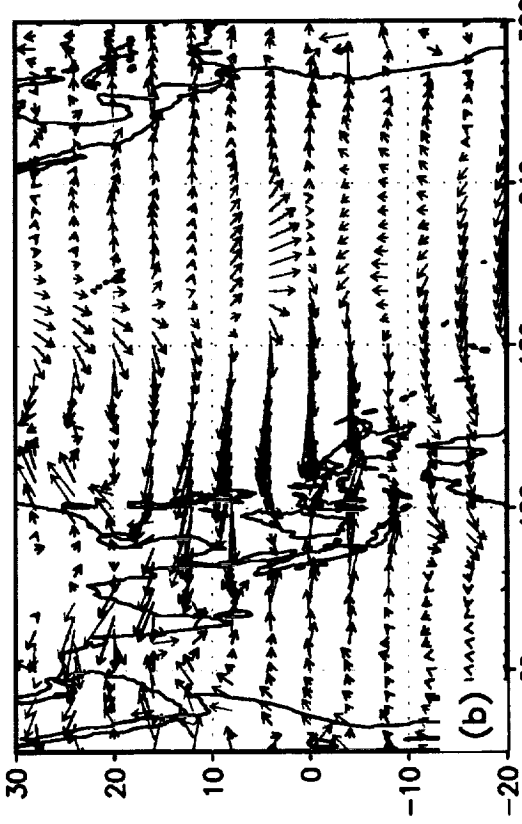
Fig. 7

July/August 1998 Anomalies
(1998)

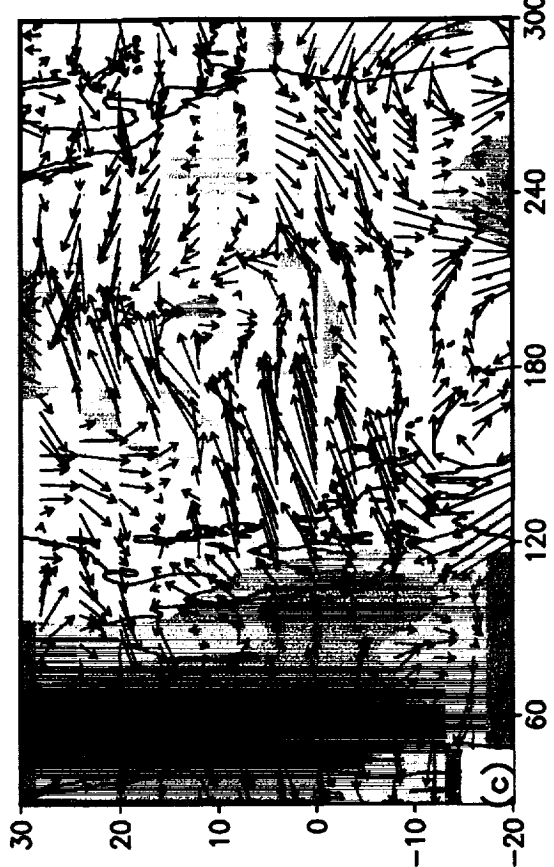
Simulation
200 hPa



850 hPa



Observations
200 hPa



850 hPa



Fig. 8

Velocity Potential at 200 hPa ($10^{-9}m^2s^{-1}$)
(1997)

Simulation May Observations May

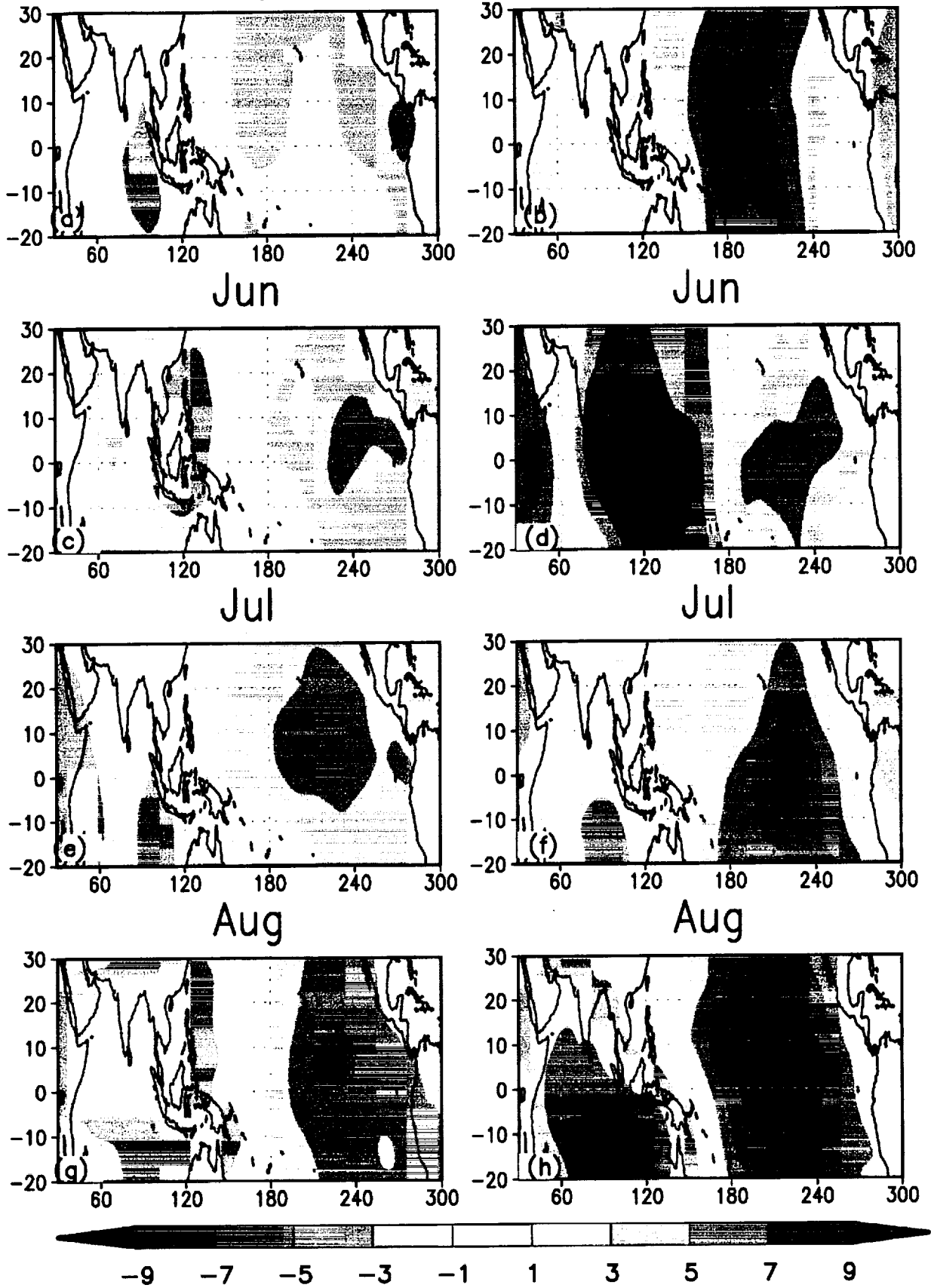


Fig. 9

Velocity Potential Anomalies at 200 hPa
(5N to 10N)

Simulation (ensemble)

Observations

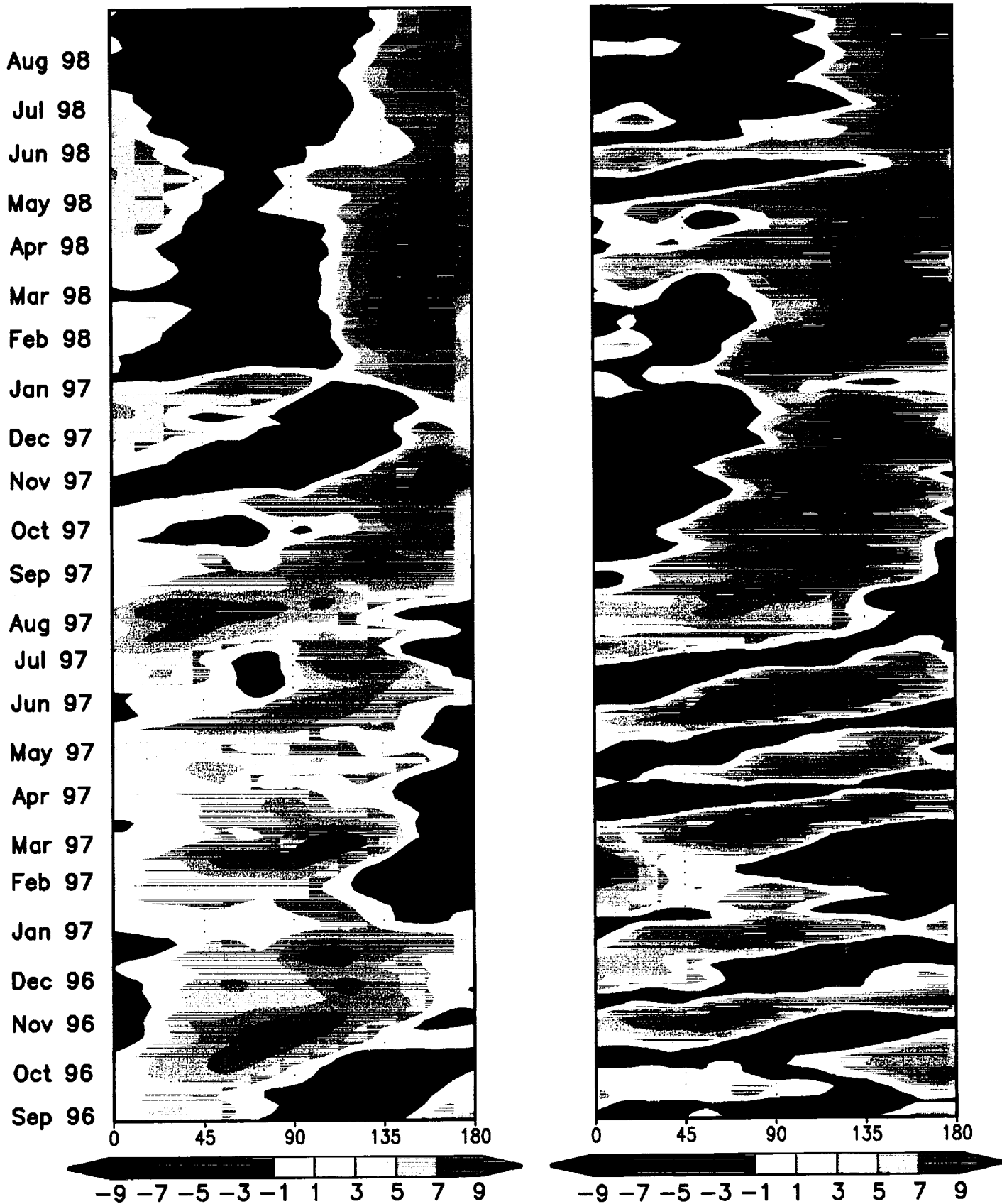


Fig. 10